Semiconductor Physics, Quantum Electronics & Optoelectronics. 2003. V. 6, N 3. P. 316-318.

PACS: 78.67.De

Many particle and bandstructure effects in intersubband quantum well optics

M.F. Pereira Jr.
NMRC, University College, Lee Maltings, Prospect Row, Cork, Ireland
Phone: +353 21 490 4178; fax: +353 21 490 4058; e-mail: mpereira@nmrc.ie.

Abstract. In this paper, intersubband optical absorption spectra are computed from an optical susceptibility derived from the many-body formalism. The theory is valid for both non-equilibrium and equilibrium conditions. Numerical results are presented for III-V quantum wells at equilibrium, and electron subband nonparabolicity is partially taken into account by means of different effective masses, adjusted to non-parabolic bands calculated with a 8×8 k·p Hamiltonian.

Keywords: quantum well, intersubband transitions, many-body formalism.

Paper received 16.04.03; accepted for publication 17.06.03.

1. Introduction

Optoelectronic devices based upon intersubband transitions create new possibilities for infrared applications. [1,2,3,4,5].

Their optical response depends mostly on the structure design, not on the material itself, and for high excitation conditions that typical devices operate, both bandstructure and many particle effects are expected to play a relevant role.

This paper presents a study of the interplay between many particle and bandstructure effects, namely carrier-carrier scattering, exchange and depolarisation, by means of an approach that can partially include the intersubband dispersion due to nonparabolicity in the conduction subbands. [6,7] The general theory supports both nonequilibrium and equilibrium cases and is based on Keldysh Greens Functions. The equilibrium results given here go beyond previous theories, which apply an ansatz where full Coulomb coupling terms are replaced by averages. [8]

In contrast to these theories, we solve our equations exactly, without making use of this ansatz, by means of a numerical matrix inversion technique that extends previous methods successfully used for conventional semiconductor lasers. [9] It is beyond the scope of this paper to give a detailed description of the formalism used. The main equations are highlighted in Section II, with numerical results given in Section III and followed by a brief summary.

2. Microscopic optical response

Optical absorption α at a given photon energy can be calculated from the imaginary part of the optical susceptibility χ,

$$\alpha(\omega) = \frac{4\pi\omega}{cn_b}\Im\{\chi(\omega)\},$$
$$\chi(\omega) = \sum_{k,l,m} \wp_{ml}\chi_{lm}(k,\omega). \qquad (1)$$

Here n_b denotes the background refractive index, $\wp_{ml}$ is the transition dipole moment between the subbands "m" and "l", and c is the speed of light. The susceptibility function, $\chi_{lm}(k,\omega)$ is related to the carriers Green's Function, G Its time evolution is described by a Dyson equation, with Coulomb interactions as well as other scattering mechanisms included in a selfenergy, Σ [10].

The carriers selfenergy includes scattering and leads to bandgap renormalization and spectral broadening, as well as exchange and depolarisation effects. Electron-electron scattering is described here within the GW approximation, with a quasi-statically-screened potential W, and the corresponding spectral broadening, $\Gamma_{lm}(k,\omega) = \Im\{\Sigma_{lm}(k,\omega)\}$, which appears in the equations that follow, is calculated at the miniband gap and at $k = 0$. The steady-state absorption spectra discussed have been numerically computed assuming the carriers are thermalized in quasi-equilibrium in the various subbands, each subband l characterised by an occupation function $n_l(k)$.

The resulting integral equation for the susceptibility function reads,

$$\hbar(\omega - e_l(k) + e_m(k) + i\Gamma_{ml}(k,\omega))\chi_{lm}(k,\omega) +$$
$$+ (n_l(k) - n_m(k))2V_0^{lmml}\sum_{\vec{q}}\chi_{lm}(\vec{q},\omega) -$$
$$-(n_l(k) - n_m(k))\sum_{\vec{q}}V_{\vec{k}-\vec{q}}^{llmm}\chi_{lm}(\vec{q},\omega) =$$
$$= \wp_{lm}(n_l(k) - n_m(k)),$$

where $V_{\vec{k}-\vec{q}}^{nmlp}$ represents the various bare Coulomb interaction matrix elements, and the renormalized energies are given by,

$$\hbar e_l(k) = \hbar\varepsilon_l(k) - \sum_{\vec{q}} n_l(q)V_{\vec{k}-\vec{q}}^{llll} + \sum_{\vec{q}} n_l(q)V_{\vec{k}-\vec{q}}^{lmml}. \qquad (3)$$

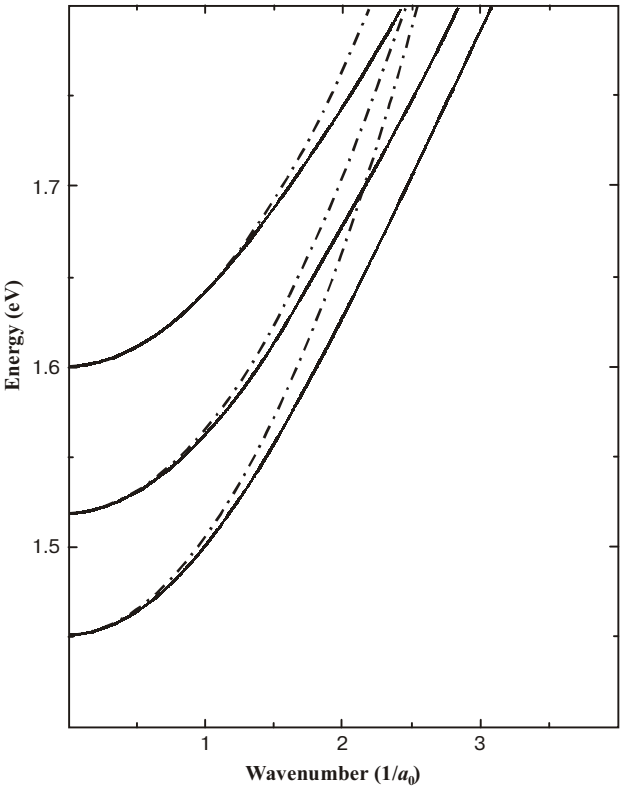

Fig. 1. First three nonparabolic electronic subbands (dotted) and corresponding parabolic fits (dot-dashed) for a 9 nm InGaAsP/GaAsP quantum well, $\hbar\varepsilon_l(k)$ that appears in Eq. 3), and a_0 = 8.55 nm is the 2D exciton Bohr radius for the corresponding quantum well material.

3. Numerical results

In all figures below, a 9 nm InGaAsP/GaAsP quantum well at T = 300 K is considered. Each nonparabolic conduction subband, obtained from a 8×8 k·p Hamiltonian, [7], is approximated by a parabolic band. From lowest to highest subband, the resulting effective masses are: m_{eff} = 0.086, 0.099, 0.112, 0.111, 0.115×m_0, where m_0 is the free electron mass. Fig. 1, depicts the first three electron subbands, together with the corresponding parabolic fits.

Dispersion originating from different effective masses plays a crucial role in the general characteristics of intersubband optical spectra. Fig. 2 illustrates the interplay between subband dispersion (due to the different effective masses adjusted to the originally non parabolic bands), and Coulomb effects through numerical solutions of Eq. 2.

The spectral shifts due to Coulomb corrections depend on the occupation of each subband, which in turn depend on the effective masses. That explains the difference in relative shifts of the different transitions seen in Figs 2a and 2b.

If the subband dispersion is sufficiently large, a sizeable increase in oscillator strength with corresponding reduction in bandwidth can occur in some transitions, as seen in Fig. 2a.

Fig. 3 shows the evolution of optical spectra with increasing carrier density. The multisubband case can lead to a very interesting dependence of optical spectra on subband occupation. Each subband is filled at a different rate due to the different effective masses and the actual occupation will influence the amount of spectral shift and increase in oscillator strength, as discussed above. The resulting optical spectra can be extremely different from those predicted by free particle theories.

It is clear that in the presence of a high density of electrons, screening of the Coulomb interaction plays an important role.

In our approach, screening appears in higher order corrections to the Hartree-Fock depolarisation and exchange terms presented here. There are both diagonal and nondiagonal corrections, which are the subject of current research. The resulting complex numerical codes necessary to implement such corrections, including nonparabolicity at various levels are under development.

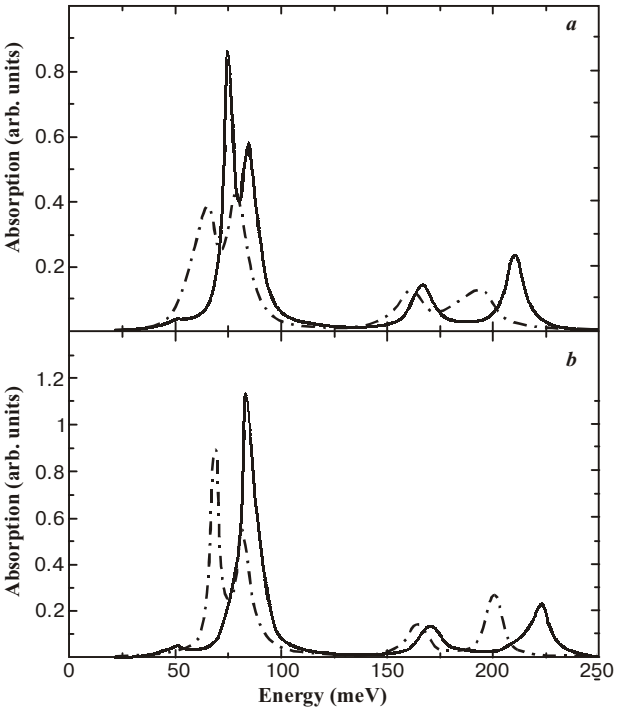

Fig. 2. Normalised intersubband absorption spectra with N = = 2.5×10^{12} carriers/cm^2. The solid and dot-dashed curves are respectively with many particle corrections, and for free carriers. Different effective masses as explained in the text are used in (*a*) while m_{eff} = 0.086 in all subbands is used in (*b*).

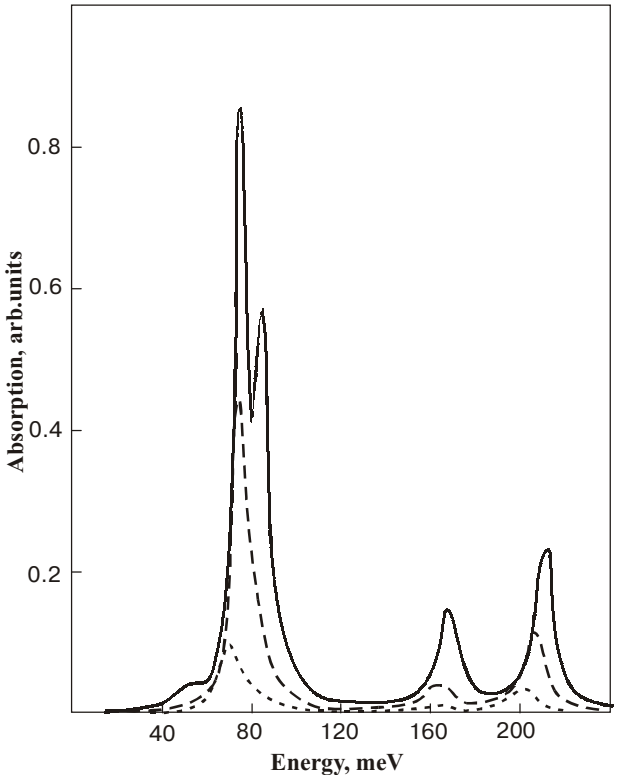

Fig. 3. Intersubband absorption for the same structure of Fig. 1. The dotted, dot-dashed and solid lines are, respectively forcarrier densities N = 0.5, 1.5 and 3×10^{12} carriers/cm^2. Many particle corrections and subband dispersion are included.

4. Conclusions

In summary, the numerical results presented show that, even at lowest level, both nonparabolicity and many particle effects are important and must be taken into account in the computation of intersubband optical spectra. Stronger deviations are expected by considering full nonparabolicity in both dispersion relations and corresponding k-dependent dipole transition moments. A new generation of numerical codes is under development to describe these effects and the limiting cases presented here are already a step forward compared to previous theories found in the literature.

The approach can be used for basic physics studies and comparisons with experiments as well as a starting point for the realistic simulation of new optoelectronic devices.

Acknowledgments

The author thanks Science Foundation Ireland (SFI) for financial support of this work and E. O'Reilly for a critical reading of the manuscript.

References

1. J. Faist, F. Capasso, A.L. Hutchinson, L. Pfeiffer and K.W. West // *Phys. Rev. Lett.*, **71**, 3573 (1993).
2. C. Sirtori, P. Kruck, S. Barbieri, P. Collot, J. Nagle, M. Beck, J. Faist, U. Oesterle // *Appl. Phys. Lett.*, **73** 3486 (1998).
3. S.-C.Lee and A. Wacker // *Physica*, **E13** 858-861 (2002).
4. S.-C.Lee and A. Wacker // *Phys. Rev.*, **B66**, 245314 (2002).
5. M.F. Pereira Jr., S.-C.Lee and A. Wacker // *Physica*, **E**, *in Press*.
6. M.F. Pereira Jr. and H. Wenzel // *Phys. Stat. Sol.*, **B232**, 134 (2002).
7. H. Wenzel, G. Erbert and P. Enders // *IEEE Journal of Selected Topics in Quantum Electronics*, **5**, 637 (1999).
8. D.E. Nikonov, A. Imamoglu, L.V. Butovand, H. Schmidt // *Phys. Rev. Lett.*, **79**, 4633 (1997).
9. M.F. Pereira Jr. and K. Henneberger // *Phys. Rev.*, **B58**, 2064 (1998).
10. L.V. Keldysh, Zh. Eksp // *Teor. Fiz.* **20**,4 (1965). [Sov. Phys. JETP **20**, 4 (1965)].